Cooperative Multi-Robot Estimation and Control for Radio Source Localization

Benjamin Charrow, Nathan Michael, Vijay Kumar

Abstract We develop algorithms for estimation and control that allow a team of robots equipped with range sensors to localize an unknown target in a known but complex environment. We present an experimental model for radio-based time-of-flight range sensors. Adopting a Bayesian approach for estimation, we then develop a control law which maximizes the mutual information between the robot's measurements and their current belief of the target position. We describe experimental results for a robot team localizing a stationary target in several representative indoor environments in which the unknown target is reliably localized with an error well below the typical error for individual measurements.

1 Introduction

Having robotic teams that are capable of quickly localizing a target in a variety of environments is beneficial in several different scenarios. Such a team can be used in search and rescue situations where a person or object must be located quickly. Cooperative localization can also facilitate localization of robots within a team towards tasks like cooperative mapping or surveillance. Given these multiple applications, it is reasonable to equip the robots with additional sensors to support localization. In this paper, we focus on the case where each robot is equipped with a range-only RF sensor. These sensors provide limited information about the state of the target, necessitating the development of an active control strategy to localize the target.

There is extensive work on algorithms for localizing stationary nodes using range sensors notably in open field environments by Kantor and Singh [8].

Benjamin Charrow, Nathan Michael, Vijay Kumar
GRASP Lab, University of Pennsylvania
e-mail: {bcharrow,nmichael,kumar}@seas.upenn.edu

Spletzer and Taylor [19] also examined a multi-node stationary localization problem for both range and bearing sensors with bounded error. Grocholsky [4] and Stump et al. [20] examined the active control question by designing controllers which maximized the rate of change of the Fisher information matrix to localize a stationary target. However, their work assumed that the belief was Gaussian distributed, which is not the case for typical range measurements.

In our paper, we present a probabilistic approach for estimating the location of a target as well as an information-theoretic control strategy which seeks to maximize the usefulness of future measurements that the team makes in the more general non-Gaussian setting. This avenue of research was pursued by Hoffman and Tomlin [5]. They showed how particle filters can be used in obstacle-free environments with non-linear sensor models to calculate mutual information. We build on their work and extend it to work in non-convex environments. We also improve on their numerical approximation of mutual information yielding more efficient and potentially better control inputs.

Ryan and Hedrick [16] also investigated information-theoretic control and developed a receding horizon controller for a single mobile robot to track a mobile target. They approximate mutual information using a randomized algorithm which does not rely on numerical integration. Our work differs by focusing on real time control inputs for multiple robots.

These approximation methods are necessary, as naïve approaches to maximize mutual information almost immediately lead to significant computational difficulties. The fundamental complexity arises from an integration that must be performed over both the state and measurement spaces. While direct numerical calculations can be used, approximation algorithms for certain distributions exist. In this work we use the approach by Huber et al. [6] for approximating the entropy of Gaussian mixture models.

Our work is also closely related to work by Olson et al. [11] and Djugash et al.[2, 3]. In these works, a single mobile robot localizes itself and the nodes in a sensor network with many nodes using range measurements. Both of their experimental results rely on manually driving the robot throughout the environment. Our work addresses the problem of how robots should move, which is necessary as we have fewer robots generating measurements.

Both our estimation and control strategies are fully centralized and require communication throughout the team. This limitation is not significant as the team's only sensor is RF-based. If the team was in an environment where they could not communicate, they could not gather measurements either.

In the rest of this paper we detail our estimation and control algorithms that enable a team of robots to successfully localize a stationary target in non-convex environments. Our primary focus is on a series of experiments that we designed to test our approach across different indoor environments and a variety of initial conditions. Overall, we are able to repeatedly localize a target with an error between 0.8-1.9m using only two robots equipped with

commercially available RF range sensors. A highlight of our work is that despite the limited information that the team has when they are at any fixed position, they are able to effectively coordinate and use their mobility so that the estimate of the target rapidly converges.

2 Technical Approach

In our approach, the robotic team maintains a distribution over possible locations of the target's location using a particle filter. The team constantly seeks to maximize the mutual information between the current estimate of the target's state and expected future measurements. Both the filter and the control directions are computed in a centralized manner.

2.1 Measurement Model

We consider the case where the team's only way of sensing the target is through a *range*-only sensor. A standard approach for building these sensors is to use the Time Difference of Arrival (TDoA) of a signal between two nodes. Because of this, any delay in the signal's propagation results in an over-estimate of the distance. Conversely, an overestimate of the signal's speed results in an under-estimation of the distance. We use the nanoPAN 5375 – a TDoA RF sensor which operates in the 2.4GHz spectrum in our experiments and show that it exhibits both positive and negative biases, which are primarily a function of whether or not the sensors are in line of sight (LOS) or non line of sight (NLOS). Our data also show that the magnitude of the bias and variance increase with the true distance between the sensors.

There is significant empirical and theoretical support for treating LOS and NLOS measurements differently [13, 12]. TDoA methods work best when radios are not obstructed by obstacles and have clear LOS conditions. However, when radios do not have LOS they are more likely to be affected by scattering, fading, and self-interference, causing non-trivial positive biases. We model the error of the measurement conditioned on the true state as:

$$p(z \mid x) = \begin{cases} \mathcal{N}(z; \alpha_0 + r\alpha, r\sigma_L^2) & \text{LOS} \\ \mathcal{N}(z; \beta_0 + r\beta, r\sigma_N^2) & \text{NLOS} \end{cases} \tag{1}$$

where r is the true distance between the sensors and $\mathcal{N}(z; \mu, \sigma^2)$ is a normal random variable with mean μ and variance σ^2. α_0 and β_0 are the biases, while α and β determine how the biases change with distance. It is straightforward to calculate the maximum likelihood estimate (MLE) of these parameters for this model with labeled data. Throughout this paper, we assume that

measurements are conditionally independent of each other given the true state (i.e. $p(z_1, z_2 \mid x) = p(z_1 \mid x)p(z_2 \mid x)$).

Models for TDoA sensors typically use a biased Gaussian with constant or time-varying variance [17, 7], whereas (1) is more similar to those used in power based range models. We have chosen this approach because, as Patwari et al. noted, the Gaussian model does not perform as well at large distances as the tails of the distribution become heavy [12]. Letting the variance increase with distance ensures that the model handles large deviations from the truth without using a Gaussian mixture model, which would increase the computational complexity of the control as we discuss later.

2.2 Estimation

Range measurements are a non-linear function of the target state and can easily lead to non-trivial multi-hypothesis belief distributions as well as rings and crescents. For these reasons, we use a particle filter for the estimation. Formally, let $\mathbf{x}_t = [x, y]$ be the state of the target at time t and $\mathbf{c}_t^i = [x, y]$ be the state of i^{th} member of the team. The full configuration of the team is $\mathbf{c}_t = [\mathbf{c}_t^1, \ldots, \mathbf{c}_t^n]$. Each robot makes a 1-d range measurement z_t^i as they move around the environment. Aggregating these measurements produces a vector $\mathbf{z}_t = [z_t^1, z_t^2, \ldots, z_t^n]$. Where appropriate, we will write $\mathbf{z}_t(\mathbf{c}_t)$ to emphasize that the measurements depend on the configuration of the team.

The belief at time t is the distribution of the state conditioned on all measurements up to time t. A typical Bayesian filter incorporates measurements over time recursively and a particle filter approximates this as a weighted sum of Dirac delta functions [21]:

$$bel(\mathbf{x}_t) = \eta\, p(\mathbf{z}_t \mid \mathbf{x}_t) \int bel(\mathbf{x}_{t-1}) p(\mathbf{x}_t \mid \mathbf{x}_{t-1}, \mathbf{u}_t)\, d\mathbf{x}_{t-1} \approx \sum_j w_j \delta(\mathbf{x}_t - \tilde{\mathbf{x}}_j) \tag{2}$$

where η is a normalization constant, $\tilde{\mathbf{x}}_j$ is the location of the j^{th} particle and w_j is its weight. While this equation is standard, we wish to emphasize that the approximation is *discrete*. As we show in Sect. 2.3, this enables approximations of mutual information.

Aside from representing complex distributions, particle filters also have the advantage that they do not require each measurement to be classified as LOS or NLOS. Assuming that the robots have a map of the environment, they can use it to determine which of the two distributions in our measurement model (1) to use on a *per particle* basis by seeing if a straight line between the particle and the robot intersects any walls.

While the standard particle filter equations allow for the incorporation of non-linear control inputs, $\mathbf{u}_t$, in our scenario the target is stationary. Despite this, in our experiments we injected noise into the system to avoid particle

degeneracy problems. Specifically, we perturbed the polar coordinates of each particle in the local frame of the robot that is making the measurement with samples from a zero-mean Gaussian distribution. We achieved the best results by rejecting samples that moved the particle more than a specified distance or caused their LOS condition to the measuring robot to change. We also used a low variance resampler when the number of effective particles dropped below a certain threshold. All of these techniques can be found in standard books on estimation (e.g. Probabilistic Robotics [21]).

2.3 Control

Our control strategy is designed to drive the team so that they obtain measurements which lead to a reduction in the uncertainty of the target estimate. The mutual information between the current belief of the target's state and expected future measurements captures this intuitive notion. The advantage of this approach is that it incorporates the current belief of the target's state along with the measurement model to determine how potential future measurements will impact the state. By design the team will move in directions where their combined measurements will be useful. This is particularly important when using sensors which provide limited information about the state of the target.

Formally, we select the next configuration for the robotic team using the following objective function:

$$\mathbf{c}_{t+1} = \arg\max_{\mathbf{c}\in\mathcal{C}} \ \mathbf{MI}[\mathbf{x}_t, \mathbf{z}(\mathbf{c})] = \arg\max_{\mathbf{c}\in\mathcal{C}} \ \mathbf{H}[\mathbf{z}(\mathbf{c})] - \mathbf{H}[\mathbf{z}(\mathbf{c}) \mid \mathbf{x}_t] \qquad (3)$$

where $\mathbf{H}[\mathbf{x}], \mathbf{H}[\mathbf{x} \mid \mathbf{z}]$ and $\mathbf{MI}[\mathbf{x}, \mathbf{z}]$ are the differential entropy, differential conditional entropy, and mutual information, respectively, as defined by Cover and Thomas [1]. The domain of the optimization problem is the configuration space of the team, $\mathcal{C}$. Different configurations of the team will affect the mutual information by affecting both entropies in (3).

2.3.1 Determining Locations

Typical indoor environments are non-convex, meaning we must maximize mutual information over a non-convex set. To do this, we propose searching over a discrete set of configurations of the team. In our experiments, we do this by creating a connectivity graph along with an embedding into the environment. At each time step, robots find candidate locations by performing breadth first search and taking nodes within specified range intervals. Short ranges allow a robot to continue gathering useful measurements where it is, while long ranges enable it explore new locations.

To create the connectivity graph we perform a Delaunay triangulation of the environment and define the incenters of the triangles as nodes. This requires a polygonal representation of the obstacles, but it is straightforward to create these from an occupancy grid map. For edges, we connect nodes from adjacent triangles as well as their transitive closure. Figure 2 shows two examples of this approach, which we used in our experiments.

2.3.2 Calculating The Objective

Hoffmann and Tomlin [5] developed an approach for calculating mutual information with particle filters that we use here. In particular, they showed that by using the particle filter's discrete approximation of the belief, (2), the entropies can be expressed as:

$$\mathbf{H}[\mathbf{z}] \approx -\int_{\mathbf{z}} \left(\sum_i w_i \; p(\mathbf{z} \mid \mathbf{x} = \tilde{\mathbf{x}}_i) \right) \log \left(\sum_i w_i \; p(\mathbf{z} \mid \mathbf{x} = \tilde{\mathbf{x}}_i) \right) d\mathbf{z} \quad (4)$$

$$\mathbf{H}[\mathbf{z} \mid \mathbf{x}] \approx -\int_{\mathbf{z}} \sum_i w_i \; p(\mathbf{z} \mid \mathbf{x} = \tilde{\mathbf{x}}_i) \log p(\mathbf{z} \mid \mathbf{x} = \tilde{\mathbf{x}}_i) d\mathbf{z} \quad (5)$$

Where we have dropped the measurement's dependence on the configuration of the team for brevity. The approximate equalities are due to the particle filter's approximation of the belief.

In our work, we further exploit the assumed conditional independence of the measurements given the state when calculating the conditional entropy. By exchanging summation and integration, we can rewrite (5) as $\mathbf{H}[\mathbf{z}(\mathbf{c}) \mid \mathbf{x}] \approx \sum_i w_i \sum_j \mathbf{H}[z_j(c_j) \mid \mathbf{x} = \tilde{\mathbf{x}}_i]$ This reduces the conditional entropy to be multiple *separate* integrals over a single measurement space – which can often be done analytically – as opposed to one integral over the joint space of all measurements the team makes.

The entropy of the measurement distribution (4) is harder to compute. However, the particle filter transforms the distribution into a finite dimensional mixture model, which enables new approximation techniques.

2.3.3 Approximating Mutual Information

Unfortunately, performing the mutual information calculations in real time for teams with more than 3 or 4 robots is computationally infeasible: evaluating the mutual information of a single configuration requires numerically integrating over the full measurement space to calculate the measurement entropy. Rather than performing numerical integration over subsets of the space [5], we view the measurement distribution $p(\mathbf{z})$ as a mixture model. The i^{th} component is $p(\mathbf{z}(\mathbf{c}) \mid \mathbf{x} = \tilde{\mathbf{x}}_i)$ with weight w_i, both of which are de-

termined by the i^{th} particle. Because our measurement model is Gaussian, we can use a deterministic approximation algorithm for evaluating the entropy of Gaussian mixture models [6].

The algorithm is based on a Taylor series expansion of the logarithmic term in the integral. This replaces the log term by a sum. Exchanging the order of integration and summation, the entropy can be expressed as a weighted sum of the Gaussians' central moments. The integrals can be calculated analytically, and only the weighting terms need to be computed online.

We only use the 0^{th}-order term in the Taylor series expansion:

$$\mathbf{H}[\mathbf{z}] \approx -\int_{\mathbf{z}} \sum_k w_k \mathcal{N}(\mathbf{z}; \mu_k, \Sigma_k) \log g(\mu_k)\, d\mathbf{z} = -\sum_k w_k \log g(\mu_k) \quad (6)$$

$g(\mu_k)$ is the likelihood of the mixture model evaluated at the mean of the k^{th} component. The computational complexity of this approximation is $O(n^2 l)$ where n is the number of particles and l is the number of robots. The time is linear in l because the conditional independence assumption in the measurement model results in the covariance matrix of the measurements being diagonal. Table 2 summarizes the computational complexity of the entire approach.

This approach also works when the measurement model is itself a mixture of Gaussians. However, this would result in one mixture component for every separate combination of mixture components from all robots, leading to exponential growth. This is partly why we use a Gaussian measurement model with distance dependent variance rather than a Gaussian mixture model.

3 Experiments

3.1 Experimental Design

There are four primary questions that we seek to answer with our experiments: 1) does our measurement model result in an accurate estimate of the target's location? 2) is mutual information an appropriate metric to maximize? 3) does our approximation of mutual information provide reasonable trajectories? 4) are our results repeatable across different environments and with various starting conditions?

We design three separate experiments to answer these questions. All of the experiments have two robots trying to locate a third stationary robot. To assess repeatability, we run 10 independent trials of each experiment. For each trial, we let the robots explore the environment without interacting with them, and only stop them once the filter reaches a stable estimate.

To evaluate the performance of each trial, we calculate the empirical mean of the filter's distribution as well as the volume of its covariance matrix (i.e.

its determinant). These statistics are not always an accurate reflection of the filter's performance (e.g. the average of two distinct hypotheses may be far from either hypothesis), but will show whether the filter accurately converges to a single estimate over time.

We use a qualitative approach to evaluate the trajectories of the robots, and manually assess whether or not they are reasonable. As a baseline comparison, in open environments with no prior knowledge of the target's location, it is best to move two range sensors orthogonally to one another as is seen in other approaches [4, 20, 11].

In Experiment 1, we place two robots within 0.5m of each other and put the target in NLOS conditions approximately 16m away. A good control strategy for this experiment will result in the robots moving in complementary directions rather than staying tightly clustered together.

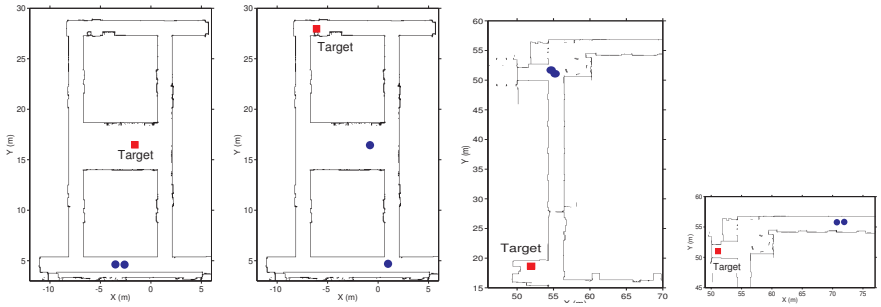

(a) Expt. 1 (Levine) (b) Expt. 2 (Levine) (c) Expt. 3 (Towne) (d) Expt. 4 (Towne)

Fig. 1: Starting configurations of robots. Blue dots show the starting location of the two mobile robots and the red square shows the location of the target.

For Experiment 2, we place the robots far away from each other to see if they still move in complementary directions. The separation also tests whether the measurement model consistently combines measurements from different modalities; if the robots follow good trajectories, they will achieve LOS to the target at different times.

In Experiment 3, we place the robots within 0.5m of each other with the target more than 30m away. Experiment 3 also takes place in a different environment. Experiments 1 and 2 take place in Levine Hall at the University of Pennsylvania, which was constructed primarily in 2003 with modern constructions materials – its walls are primarily made up of wood or metal framing with drywall. Experiments 3 and 4 take place in Towne Building which was built in 1906 – its walls are typically made of brick or concrete.

For experiment 4, we again place the robots close to each other with the target 20m along a hallway that has a slight bend. Raycasts from the robots to the target barely intersect a wall, making it ambiguous whether or not the

RF signal will exhibit LOS or NLOS behavior. Figure 1 shows the starting location of the target and robots for each experiment.

3.2 Equipment and Configuration

We use simple differential drive robots equipped with Hokuyo-URG04LX laser scanners and 802.11s wireless mesh cards for communication. The experimental software is developed in C++ and interfaced via Robot Operating System [14]. The range sensor is commercially available as part of the nanoPAN 5375 Development Kit [10]. The target remains stationary for the duration of each trial while the mobile robots are limited to a maximum speed of $0.2\frac{\mathrm{m}}{\mathrm{s}}$. The particle filter and mutual information calculations are performed on a laptop with 4GB RAM and an Intel Core Duo processor. To prevent collisions between the mobile robots, we use the Optimal Reciprocal Collision Avoidance algorithm provided in the RVO2 library [18, 15].

For localization, planning, and determining LOS conditions we use a known occupancy grid map of the environment with a resolution of 0.05m. The results of the triangulation algorithm in Sect. 2.3.1 are shown in Fig. 2. Robots consider nodes within 1.0-2.0m or 8.0-9.0m of their current location for the control update, which typically result in 7-12 locations per robot.

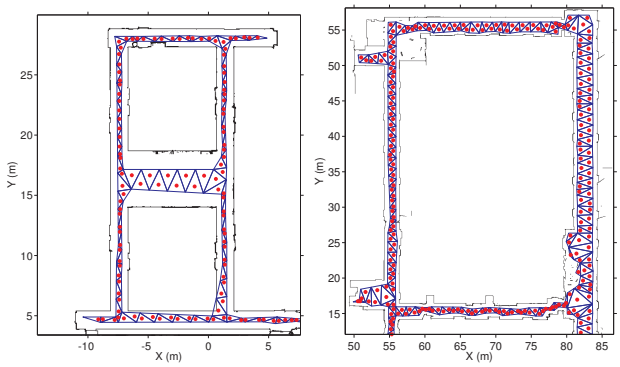

(a) Levine Triangulation (b) Towne Triangulation

Fig. 2: Graphs for candidate locations. Delaunay triangles are shown along with their incenters which form the vertices of the graph.

We uniformly sample 2500 locations throughout the environment to initialize the particle filter and run a low variance resampler when the proportion of effective particles drops below 0.3. We calculate the MLE of the measurement model's parameters, (1), using a separate dataset gathered in

	LOS	NLOS
α_0, β_0	2.51	-1.34
α, β	0.20	-0.24
σ_L^2, σ_N^2	7.00	14.01

Table 1: Measurement Model Parameters.

Task	Cost
Single Evaluation	$O(n^2 l)$
Solving Objective	$O(n^2 l d^l)$

Table 2: Computational complexity of control law (3) with n particles, l robots, and d potential locations per robot.

Levine. During the experiments, we double the MLE variances to prevent the filter from prematurely converging without affecting the location of the convergence. Specifically, if $\sigma_{L,\text{MLE}}$ and $\sigma_{N,\text{MLE}}$ are the MLE values of the variance for LOS and NLOS conditions, we set $\sigma_L = 2\sigma_{L,\text{MLE}}$ for LOS and $\sigma_N = 2\sigma_{N,\text{MLE}}$ for NLOS. Parameter values for the experiments are listed in Table 1. We emphasize that the parameters are equivalent for *both* the Towne and Levine experiments.

3.3 Results

Figure 3 shows the error of the nanoPAN 5375's measurements as a function of distance. At short distances in LOS conditions the nanoPAN provides consistent measurements with an error larger than 2.0m. In NLOS conditions there is significant variability in both the mean and variance of the measurements as the distance between source and receiver increases. This data helps justify our choice of measurement model as it is clear that LOS and NLOS conditions have different sensor measurement biases and variances.

Overall, our approximation of mutual information resulted in good trajectories for the robots. Figure 4 shows that the robots moved to gain complementary measurements; they moved orthogonally to one another when possible, and once they had localized the source, they maintained LOS. Figure 5 shows this process in more detail. Initially, both robots moved away from each other. Next, the robot on the left moved up the vertical hallway, while the other robot moved laterally; an orthogonal movement pattern. Once measurements along the horizontal hallway were no longer helpful due to the symmetry of the distribution, Fig. 5b, both robots moved up the vertical hallway, which caused the filter to converge. We stress that these behaviors arose organically from our objective.

Figure 5 also serves as a good example of the types of distributions that typical parametric approaches that assume a unimodal distribution cannot reliably track as there are clearly multiple equally valid hypotheses.

Figures 6 and 7 show the mean and covariance of the estimate over time across all trials and experiments. Except for Experiment 4, the mean con-

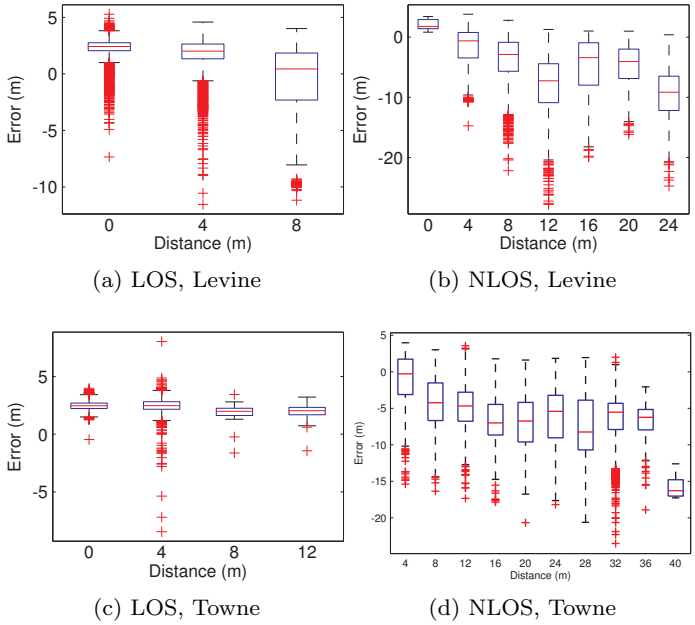

(a) LOS, Levine (b) NLOS, Levine

(c) LOS, Towne (d) NLOS, Towne

Fig. 3: Error of nanoPAN range measurements in LOS and NLOS conditions. The subfigures show standard box-plots with outliers marked as +'s. Each plot contains approximately 10,000 data points. NLOS conditions are significantly noisier than LOS conditions with statistics that vary with distance.

verged to the true state of the target, ultimately surpassing the baseline accuracy of an individual measurement in LOS conditions. Table 3 provides the resulting root mean square error (RMSE) of the converged filter. The slightly increased error in Experiment 3 suggests that the parameters for the measurement model are not exactly the same as in Levine. However, the overall error is still low. The fact that the covariance decreases and ends in the range $[-3, 0]$ on a natural logarithmic scale, shows that filter consistently converges to a single hypothesis. For reference, the natural logarithm of the determinant of the identity matrix (i.e. 1 meter variance in only x and y) has a value of 0. The consistent trends across all trials and experiments demonstrate that the fundamental approach is robust to various starting conditions and changes in the sensor across environments.

Experiment 4 is the exception to this general trend. In all 3 trials, the filter converged to a single estimate that was 5.5m away from the target's true location. The essential problem is that at the start of the experiment, raycasts in the environment between a robot and particles near the target intersect a wall, but the RF interference is low. As Figure 8a shows, the measurements exhibit negative bias and relatively low variance which are

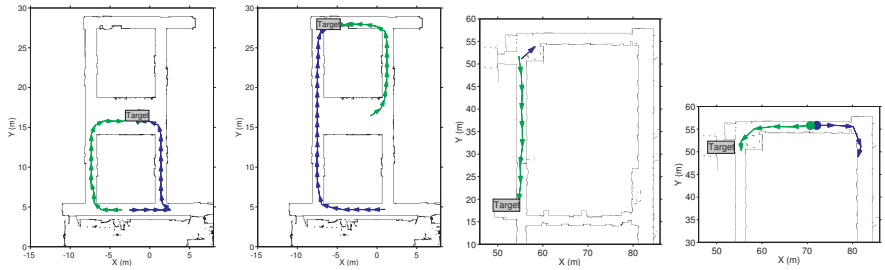

(a) Expt. 1 (Levine) (b) Expt. 2 (Levine) (c) Expt. 3 (Towne) (d) Expt. 4 (Towne)

Fig. 4: Trajectories from maximizing mutual information. Each subfigure is a typical trajectory from each experiment. The robots move to gather complementary measurements, causing the estimate of the target to converge.

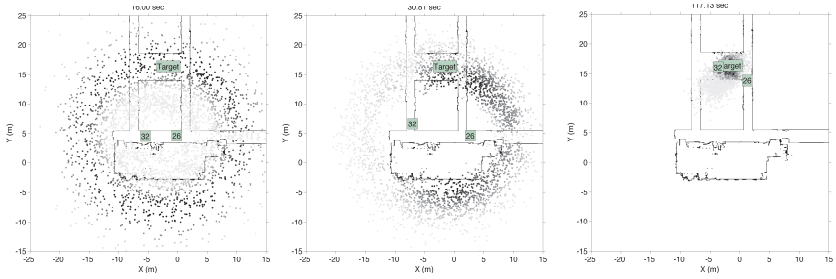

(a) $t = 16.00$ (b) $t = 30.81$ (c) $t = 117.13$

Fig. 5: Evolution of the particle filter and the robots' movement in Experiment 1. Darker particles have higher weight; a robot's position is shown by a box. a) Early range measurements cause a ring. b) Both robots move laterally, generating two hypotheses. c) The robots move up, and the filter converges.

more consistent with LOS conditions. This highlights the difference between geometric LOS and RF LOS. It is worth noting that the robots still follow a reasonable trajectory; this experiment is *not* a failure of the control.

Figure 8 shows two additional datasets from Levine which exhibit the same phenomena. Figure 8b shows a dataset gathered by having a robot drive up and down a long hallway with a target at one end. The robot and target had geometric LOS for the entire time. Figure 8c shows a dataset where a robot drove along a short hallway with a target just around the corner. The robot only had geometric LOS at one end of the hallway. In both of these experiments, geometric LOS was not always equivalent to RF LOS, highlighting the need for a different approach to classifying measurements.

Expt. #	Time (s)	Mean RMSE (m)	Std. Dev. of RMSE (m)
1	140-160	0.83	0.23
2	230-250	0.87	0.46
3	280-300	1.94	0.41
4	130-150	5.79	0.11

Table 3: RMSE of converged filter across trials.

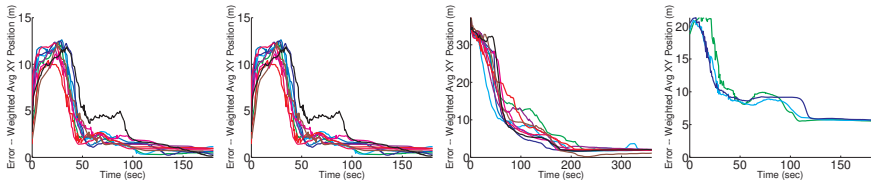

(a) Expt. 1 (b) Expt. 2 (c) Expt. 3 (d) Expt. 4

Fig. 6: Distance from weighted average of particles to target location. Each plot shows 10 trials. Except for Experiment 4, the filter converges with an error below 2m, which is below the median error of the range measurements.

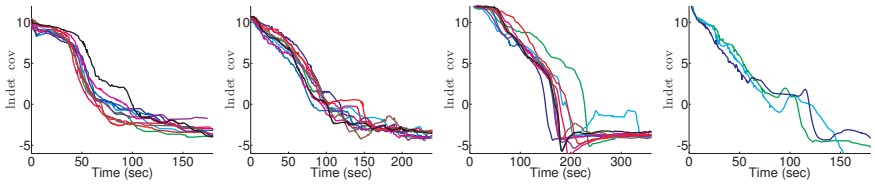

(a) Expt. 1 (b) Expt. 2 (c) Expt. 3 (d) Expt. 4

Fig. 7: Natural logarithm of the determinant of covariance. The spread of the particles decreases over time, showing the filter converges to a single estimate.

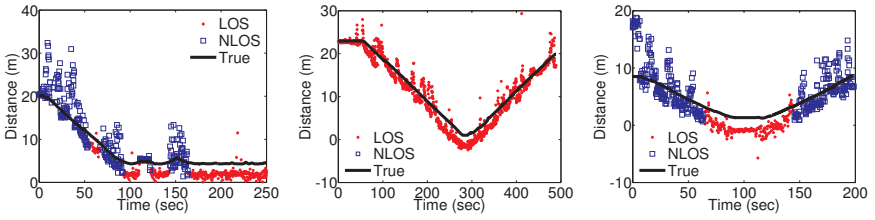

(a) Expt 4. (Towne) (b) Long Hallway (Levine) (c) Short Hallway (Levine)

Fig. 8: RF vs. Geometric LOS. These subfigures show measurements labeled as LOS or NLOS according to a raycast from the robot to the target location. Geometric LOS does not always accurately predict the negative bias and comparatively low variance of RF LOS measurements.

4 Future Work

We are currently exploring various methods for classifying measurements as LOS / NLOS. Our preliminary results suggest that latent variable methods like Hidden Markov Models (HMM) will not have the same problems as our geometric method. Morelli et al. [9] previously used a similar approach to localize a mobile beacon with more than 3 static nodes.

We are also interested in determining how well our approximation of mutual information scales, both as the number of targets increases and as the size of the robotic team increases. Longer term, we would like to extend our methods to track the state of mobile targets.

5 Conclusion

In this paper we described an active control strategy which leverages the current estimate of the target's state and knowledge of the sensor model to direct a team of robots towards locations where they will make informative measurements. We showed how approximations for the entropy of Gaussian mixture models can be used to calculate the necessary control inputs in real time. Most importantly, we presented extensive experimental results where a pair of robots successfully and repeatedly localize a target in non-convex indoor environments using commercially available RF-based range sensors. An implementation of our approach is available from the first author's website at `http://www.seas.upenn.edu/~bcharrow`

6 Acknowledgments

We gratefully acknowledge the support of AFOSR Grant FA9550-10-1-0567, ONR Grant N00014-07-1-0829, and ARL Grant W911NF-08-2-0004. The first author was supported by a NDSEG fellowship from the Department of Defense.

References

[1] T. M. Cover and J. A. Thomas. *Elements of Information Theory*. Wiley Online Library, 2004.

[2] J. Djugash and S. Singh. Motion-aided network slam. In *Proc. of the Intl. Sym. on Exp. Robot.*, New Dehli and Agra, India, December 2010.

[3] J. Djugash, S. Singh, G. Kantor, and W. Zhang. Range-only SLAM for robots operating cooperatively with sensor networks. In *Proc. of the IEEE Intl. Conf. on Robot. and Autom.*, pages 2078–2084, Orlando, USA, 2006.

[4] B. Grocholsky. *Information-theoretic control of multiple sensor platforms*. PhD thesis, University of Sydney, Sydney, Australia, 2002.

[5] G. M. Hoffmann and C. J. Tomlin. Mobile sensor network control using mutual information methods and particle filters. *IEEE Trans. Autom. Control*, 55(1):32–47, 2010.

[6] M. F. Huber, T. Bailey, H. Durrant-Whyte, and U. D. Hanebeck. On entropy approximation for gaussian mixture random vectors. In *Multisensor Fusion and Integration for Intelligent Systems*, pages 181–188, Seoul, Korea, 2008.

[7] D. Jourdan, J. Deyst, M. Win, and N. Roy. Monte carlo localization in dense multipath environments using UWB ranging. In *IEEE Intl. Conf. on Ultra-Wideband*, pages 314–319, Zurich, Switzerland, Sept. 2005.

[8] G. Kantor and S. Singh. Preliminary results in range-only localization and mapping. In *Proc. of the IEEE Intl. Conf. on Robot. and Autom.*, volume 2, pages 1818–1823, Washington, D.C., 2002.

[9] C. Morelli, M. Nicole, V. Rampa, and U. Spagnolini. Hidden markov models for radio localization in mixed LOS/NLOS conditions. *IEEE Trans. Signal Process.*, 55(4):1525–1542, 2007.

[10] nanoPAN 5375 Development Kit. `http://www.nanotron.com/EN/PR_tools.php#03`, February 2012.

[11] E. Olson, J. J. Leonard, and S. Teller. Robust range-only beacon localization. *IEEE J. Oceanic Eng.*, 31(4):949–958, October 2006.

[12] N. Patwari, J. N. Ash, S. Kyperountas, A. O. H. III, R. L. Moses, and N. S. Correal. Locating the nodes: cooperative localization in wireless sensor networks. *IEEE Signal Process. Mag.*, 22(4):54–69, 2005.

[13] T. S. Rappaport. *Wireless Communications: Principles and Practice*. Prentice Hall, 1996.

[14] Robot Operating System. `http://www.ros.org/wiki/`, February 2012.

[15] RVO2 Library. `http://gamma.cs.unc.edu/RVO2/`, February 2012.

[16] A. Ryan and J. K. Hedrick. Particle filter based information-theoretic active sensing. *Robotics and Autonomous Systems*, 58(5):574–584, 2010.

[17] B. M. Sadler, N. Liu, Z. Xu, and R. Kozick. Range-based geolocation in fading environments. In *Allerton Conf. on Comm., Control, and Comput.*, pages 15–20, Allerton House, USA, 2008.

[18] J. Snape, J. van den Berg, S. J. Guy, and D. Manocha. Smooth and collision-free navigation for multiple robots under differential-drive constraints. In *Proc. of the IEEE/RSJ Intl. Conf. on Intell. Robots and Syst.*, pages 4584–4589, Anchorage, USA, 2010.

[19] J. Spletzer and C. J. Taylor. A bounded uncertainty approach to multi-robot localization. In *Proc. of the IEEE/RSJ Intl. Conf. on Intell. Robots and Syst.*, volume 2, pages 1258–1265, Las Vegas, USA, October 2003.

[20] E. Stump, V. Kumar, B. Grocholsky, and P. M. Shiroma. Control for localization of targets using range-only sensors. *Intl. J. Robot. Research*, 28(6):743–757, June 2009.

[21] S. Thrun, W. Burgard, and D. Fox. *Probabilistic Robotics*. MIT Press, 2008.